

Few-shot Domain Adaptation for IMU Denoising

Feiyu Yao[†], Zongkai Wu^{†*}, Zhenyu Wei and Donglin Wang^{*}

Abstract—Different application scenarios will cause IMU to exhibit different error characteristics which will cause trouble to robot application. However, most data processing methods need to be designed for specific scenario. To solve this problem, we propose a few-shot domain adaptation method. In this work, a domain adaptation framework is considered for denoising the IMU, a reconstitution loss is designed to improve domain adaptability. In addition, in order to further improve the adaptability in the case of limited data, a few-shot training strategy is adopted. In the experiment, we quantify our method on two datasets (EuRoC and TUM-VI) and two real robots (car and quadruped robot) with three different precision IMUs. According to the experimental results, the adaptability of our framework is verified by t-SNE. In orientation results, our proposed method shows the great denoising performance.

I. INTRODUCTION

Inertial measurement unit (IMU) plays great importance in robotics. It consists of a gyroscope, which senses angular velocities, and an accelerometer, which can measure linear acceleration signals on three axes in space. Both angular velocities and accelerations are crucial for robotics.

Nowadays, the rapid development in robotics proposes higher demand for IMU. For example, same IMU may need to adapt to different robots or different IMUs can employ same parameters for calibration. And IMU noise problems is very serious since robots usually use low-cost IMU. The demands can be summarized as dealing gyroscope noise from multiple domains (different IMUs and different robotics). Although different methods are proposed for denoising gyroscope, from nonlinear filter methods [1], [2] and [3] denoising the IMU signal using filters to neural network methods [4], [5] and [6], they just perform well in one specific domain or need sufficiently broad range of motions to realize generalization. Recently a lot of works on few-shot learning has been done to alleviate generalization problem [7], [8]. However, these works can hardly deal with long-sequence, low-dimensional and high-variant IMU measurements.

In order to solve this problem, we propose a few-shot domain adaptation IMU denoising framework. This contains an embedding module, a restructor module and a generator module. The framework projects the IMU sequence into high-dimensional representation by embedding module and



Fig. 1. IMU is mounted on various devices: from phones and cars in daily life to unmanned aerial vehicles, Quadruped robots, ships in industry.

then use the generator to generate accurate velocities noise and bias. The restructor along with reconstitution loss is employed for embedding module to learn better representation. The framework also contains few-shot domain adaptation strategy to adapt the new domain. It employed tasks from multiple domains to update embedding module parameters by few-shot training method. This equips the model with the following ability: 1) High accurate motion information can be achieved through our denoising framework. 2) High accurate performance can be transferred to multiple IMUs and robots without readjusting.

The main contributions of this work are as followed:

- We present a few-shot domain adaption framework with embedding module, restructor nodule and generator module, which can effectively achieve accurate angular velocity error among multiple IMUs and robots without specially training the parameters for each of them.
- We propose a few-shot domain adaptation strategy for IMU sequence denoising. This strategy helps accelerate the learning process and improve its generalization ability.
- We implement our denoising method both on open dataset (EuRoC and TUM-VI) and two real robot (car and Quadruped robots) with multiple IMUs. The performance verifies the effectiveness of our method.

II. RELATED WORK

A. IMU Signal Denoising

IMU has gyroscope noise which is made up of inherent noise, linear vibration and misalignment errors. Referring to [1], these parts are related to not only IMU itself, but also the domain in which it is used (such as the robotics

[†] Contributed equally. ^{*} Corresponding author.

Z. Wu, Z. Wei and D. Wang are with Machine Intelligence Lab (MiLAB), School of Engineering, Westlake University, Hangzhou 310024, China, and Institute of Advanced Technology, Westlake Institute for Advanced Study, Hangzhou 310024, China. F. Yao is Columbia University student and works on this project as visiting students at MiLAB, Westlake University. E-mail: {yaofeiyu, wuzongkai, weizhenyu, wangdonglin}@westlake.edu.cn, feiyu.yao@columbia.edu

mechanical structure, tasks and environments). So IMU noise differs among domains.

[1] and [3] are conventional IMU signal denoising methods choosing suitable filters to denoising IMU signal. [1] takes two steps to improve the precision. First, sophisticated dynamics models is established, considering earth self rotation, measurement bias, and system noise. Then it applies a sigma Kalman filter for system state estimation. [3] employs Savitzky-Golay filters and can achieve great denoising performance with little computations time.

[4] and [6] are different from conventional methods. Artificial neural network is applied. [4] views IMU signal as time series and filters it by using Long Short Term Memory (LSTM) Recurrent Neural Network (RNN). [6] analyzes the combination between IMU denoising and RNN. It uses four different ways to analysis and finds that each performs well in specific denoising task. The artificial neural network method seems to perform well but still cannot generalize to many domains and needs plenty of labeled data.

B. Few-shot Learning

The pursuit of few-shot learning is to train a model with the "learning to learn" ability. So the model uses just small amount of training samples to learn and can handle tasks in new domain. A remarkable work in few-shot learning is MAML [9]. In this work, the parameters are trained so that it can generalize well to new domain tasks with just a small number of gradient steps with a small amount of training samples from that task. To gain this, the sensitivity of the loss functions of new domain tasks with respect to the parameters is maximized in the learning process. MAML is model-agnostic so it can be applied in many learning problems such as classification, regression and reinforcement learning. And [10], [11], [12], [13] and [14] all prove that MAML has great performance and can be generalized to many models theoretically.

[15] and [16] makes some attempts in applying few-shot learning in image denoising. The former proposes a model which is meta-trained using known synthetic noise models. The trained model can performs well with real noise after just being fine-tuned with small real training set. In this work, model is meta-trained in small training sets of synthetically generated data. So the model can generate infinite number of training tasks and the learning process only needs small training sets. These contribute to the good generalization. The latter attempts to combine meta-learning with conventional denoising methods. In this work, the model is trained through conventional methods and meta-learning enables quick adaptation of model parameters to the input when testing. Thus the model can employ with state-of-the-art denoising networks and achieve better performance.

III. FEW-SHOT DOMAIN ADAPTATION

The error characterises of gyroscope differ among multiple IMUs on multiple robots. We define them as different domains. As described by the framework in Fig. 2, The domain adaptation method we propose has three

parts: embedding module, restructor module and generator module. The embedding module achieves high dimensional representations for IMU sequence. Then the restructor is designed to reconstruct IMU sequences for better representations. The generator can output angular velocity noises in different domains without specifically tuning parameters for that domain. Here the restructor and the generator have the same neural network structure. Besides, a few-shot training strategy is also applied to help embedding module efficiently adapt to multiple domains. In this section, firstly, the task is formalized. Then key modules in our framework are introduced, which is followed by the embedding module and its training method. At last, the structure of generator is introduced.

A. Task Formulation

Given noisy and biased IMU measurements of angular rate and acceleration, our domain adaptation method is to denoise accurate angular velocity in multiple domains without further updating any parameter.

We consider specific domain tasks T made up by IMU sequences from multiple domains. The measurement of acceleration is represented as \mathbf{a}_n and the noisy and biased measurement of gyroscope is expressed as ω_n . The estimated angular rate is $\hat{\omega}_n$. The real angular rate is $\tilde{\omega}_n$.

B. Embedding, Restructor and Generator module

The embedding module creates representations where the data distributions difference among multiple domains are similar. The embedding module structure is Multi-Layer Perception (MLP)

The restructor module and the generator module have the same structure. After being latent represented by embedding module, IMU measurements should go through generator module to generate accurate angular velocities noise and bias.

Referring to [17], we can model the noise-free angular rate as:

$$\hat{\omega}_n = \hat{\mathbf{C}}_\omega \omega_n^{\text{IMU}} + \tilde{\omega}_n \quad (1)$$

Here, the intrinsic parameters $\hat{\mathbf{C}}_\omega = \hat{\mathbf{S}}_\omega \hat{\mathbf{M}}_\omega \in \mathbb{R}^{3 \times 3}$. The gyro bias $\hat{\omega}_n = \hat{c}_n + \hat{b}_n$, in which \hat{c}_n is a time-varying variable and \hat{b}_n is static bias. So we need to compute $\hat{\omega}_n$ and $\hat{\mathbf{C}}_\omega$. Notice that they have the above relations and the IMU won't change in a task. So if one is accurately estimated, the other can be optimized. Thus we apply neural network to estimate $\hat{\omega}_n$. For $\hat{\mathbf{C}}_\omega$, we initialize it as a unit matrix $I \in \mathbb{R}^{3 \times 3}$ and then optimize it during the training process.

Inspired by [18] and [17], we employ the dilated neural network structure:

$$\tilde{\omega}_n = f(\mathbf{u}_{n-N}^{\text{IMU}}, \dots, \mathbf{u}_n^{\text{IMU}}), \quad (2)$$

where $\mathbf{u}_n^{\text{IMU}} = \begin{bmatrix} \omega_n^{\text{IMU}} \\ \mathbf{a}_n^{\text{IMU}} \end{bmatrix}$. The N represents the length of local window of previous measurements, which is the base of correction for current state. $f(\cdot)$ is the function defined by neural network, which has dilated convolutions strategy.

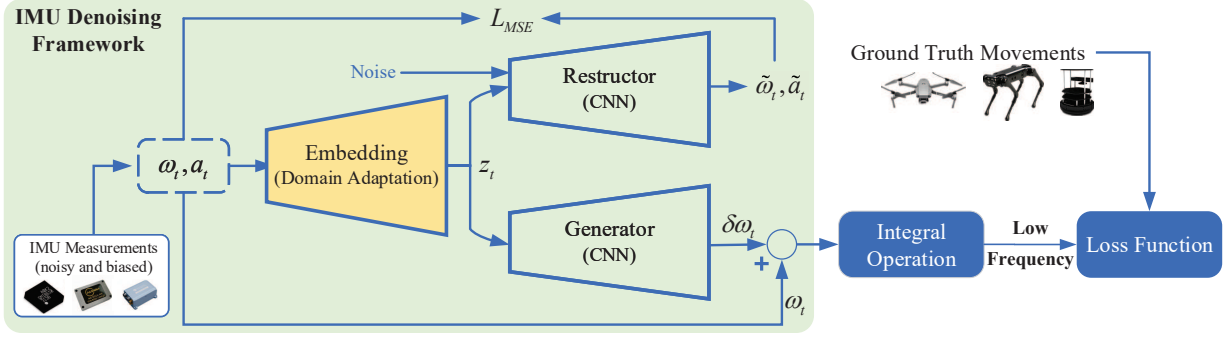


Fig. 2. Framework of our method, we divide the framework into three modules: (1) an embedding module; (2) a restructor to help embedding; (3) a generator to denoising. The embedding module is learned through few-shot learning

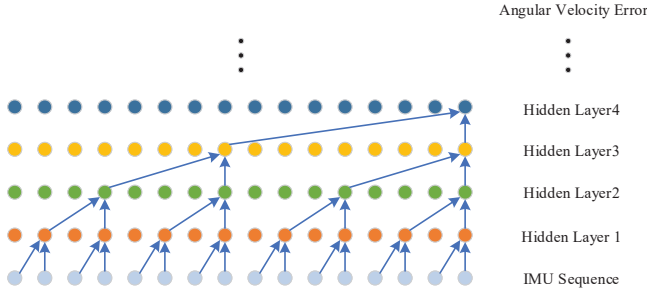


Fig. 3. Restructor and Generator module structure sketch map

Thus it can correct the data smoothly and extract time multi-scale information.

As Fig. 3 represents, in each layer, the data is handled with dilation gaps. The dilation gap in hidden layer 1 is 1. The dilation gap in hidden layer 1 is 2. In generator structure, we have 5 layers with dilation gap 1, 4, 16, 64, 1 separately. The kernel dimensions for each layer are all 7.

For the loss function, as [17] mentions, it is not suitable to use mean-square error since tracking system performance relates to frequency. Thus we apply rotate matrix to build loss function:

$$L_j = \sum_i \rho(\log(\delta \mathbf{R}_{i,i+j} \delta \hat{\mathbf{R}}_{i,i+j}^T)) \quad (3)$$

in which logarithm map $\text{SO}(3)$ is $\log(\cdot)$ and Huber loss $\rho(\cdot)$ are contained. The $\delta \mathbf{R}_{i,i+j}$ is defined as:

$$\delta \mathbf{R}_{i,i+j} = \mathbf{R}_i^T \mathbf{R}_{i+j} = \prod_{k=i}^{i+j-1} \exp(\omega_k) \quad (4)$$

The parameter j is used to reduce the frequency of IMU. The loss with different parameter j can be added to achieve the final loss in order to gain better performance.

C. few-shot training strategy

Since in real life, labelling data is quite time-consuming and laborious. For better representation with limited data, a few-shot training strategy is applied to learn the domain invariant representation z . Referring to MAML [9] structure in few-shot tasks, we apply meta-training methods to train

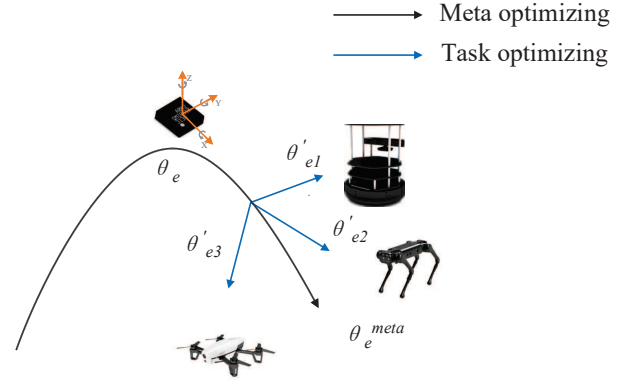


Fig. 4. Diagram of our few-shot training strategy, which optimizes the parameter θ_e using data from different robots.

embedding module suitable for multiple domains. Here comes the training method especially for embedding module.

We represent the framework G by two parameterized function f and h . f represents the reconstruction process and h represents the angular velocity error generating process. We use parameters θ_e , θ_r and θ_g to represent the embedding module, restructor module and generator module separately. Thus f has parameters θ_e and θ_r while h has parameters θ_e and θ_g . The parameterized function is a structure which applies a sequence of noised angular rate W_n and a sequence of acceleration A_n as inputs. The updated model parameters are represented as θ'_i when the new task τ_i comes.

There are two kinds of training methods in the framework: The embedding module is trained through a meta-learning method. The restructor and generator are trained through gradient method. We will specialize the training process for embedding module as followed:

In a training phase for task τ_i , there are n length angular rate sequence W_n^i , n length angular acceleration sequence A_n^i and n length ground truth angular angular rate sequence $W_{real_n}^i$. The target is to obtain the meta parameters θ_e^{meta} by few-shot training and two parameters θ_r and θ_g by normal gradient descent. Few-shot training phase is made up by two phases: adaption optimizing phase and meta optimizing phase. These two phases use different IMU sequences set τ_1

Algorithm 1 few-shot learning strategy

Input: Sequence set T containing different domain sequences $\tau_1^d, \tau_2^d, \dots, \tau_n^d$, each with IMU data and labeled data. $\theta_e, \theta_r, \theta_g$: random initialized model parameters. α and β : hyper-parameters;

Output: Meta-learned embedding module parameter θ_e^{meta} , Restructor module θ_r and Generator module θ_g ;

```

1: while not done do
2:   Sample batch sequences set  $\tau$  from  $T$ 
3:   Partition the sequences set  $\tau$  into  $\tau_1$  and  $\tau_2$ 
4:   for all  $\tau_1$  do
5:     Achieve  $\theta'_{ei}$  using:  $\theta'_{ei} = \theta_e - \alpha \nabla_{\theta_e} L_{\tau_{1i}}(G)$ ;
6:   end for
7:    $\theta_{e,g,r} = \theta_{e,g,r} - \beta \nabla_{\theta_{e,g,r}} \sum_{\tau_i \sim \tau_2} L_{\tau_{2i}}(G_{\theta'_{ei}, \theta_g, \theta_r})$ ;
8: end while
9:  $[\theta_e^{meta}, \theta_g, \theta_r] = \theta_{e,g,r}$ 

```

and τ_2 from same distribution.

When adapting to a new domain, the embedding module parameters θ_e update into θ'_e . The parameter θ_e is updated by the following gradient descent for several times.

$$\theta'_{ei} = \theta_e - \alpha \nabla_{\theta_e} L_{\tau_{1i}}(G), \quad (5)$$

in which θ'_{ei} is the updated model parameters in task τ_{1i} . α is the fixed hyper-parameter. $L_{\tau_{1i}}(G)$ has two kinds of loss from feature extractor structure and denoise structure separately:

$$L_{\tau_{1i}}(G) = L_{\tau_{1i}}^f(f) + \gamma L_{\tau_{1i}}^d(h), \quad (6)$$

in which γ is hyper-parameter. $L_{\tau_{1i}}^f$ is the reconstitution loss of for feature extractor structure:

$$L_{\tau_i}^f(f) = \sum_{W_n^i, A_n^i, \tilde{W}_n^i \sim \tau_i} \|f(W_n^i, A_n^i) - \tilde{W}_n^i\|_2^2 \quad (7)$$

$L_{\tau_{1i}}^d$ is the loss which will be introduced in the denosing structure.

In meta optimizing phase: The model employs the rest data pairs, which are W_n, A_n and \tilde{W}_n . The model parameters θ_e is updated also through gradient descent, which means:

$$\theta_{e,g,r} = \theta_{e,g,r} - \beta \nabla_{\theta_{e,g,r}} \sum_{\tau_{2i} \sim \tau_2} L_{\tau_{2i}}(G_{\theta'_{ei}, \theta_g, \theta_r}) \quad (8)$$

Here θ'_{ei} are the updated model parameters mentioned in the adaptation optimizing phase and β is a fixed hyper-parameter. $L_{\tau_{2i}}(G)$ is the loss in sequence set τ_2 . θ_e is updated through meta-training method while θ_r and θ_g are updated through gradient descent method.

After being updated through all several training phases, the final updated model parameters is the meta-trained model parameter θ_{meta} . The whole training algorithm is outlined in Algorithm 1.

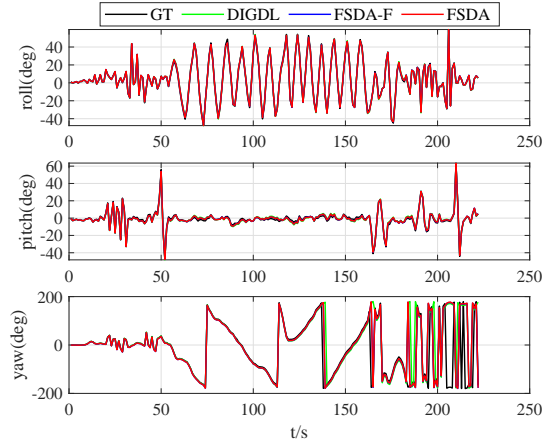


Fig. 5. Orientation estimates on the test sequence room4 for different methods.

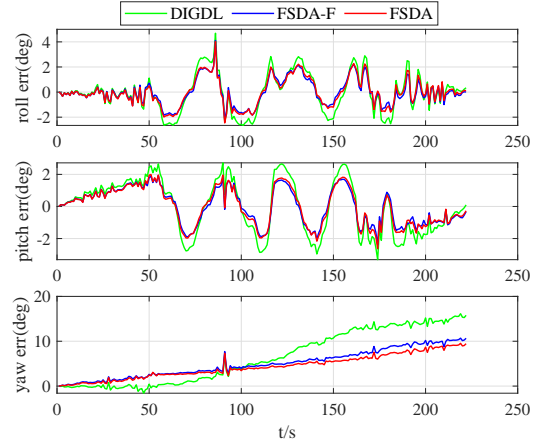


Fig. 6. Orientation errors on the test sequence room4 for different methods.

IV. EXPERIMENT RESULTS

A. Experiment Setup

To illustrate the priority of our method, we apply it in public datasets: *EuRoC* [19] and *TUM-VI* [20]:

- *EuRoC*: The data comes from a micro aerial vehicle (MAV) equipped with not calibrated ADIS16448 IMU. This dataset is composed by eleven sequences: MH 01 easy, MH 02 easy, MH 03 medium, MH 04 difficult, MH 05 difficult, V1 01 easy, V1 02 medium, V1 03 difficult, V2 01 easy, V2 02 medium and V2 03 difficult. MH is for industrial machine hall. V1 and V2 is for vicon room but V2 is created more than three months later. Easy, medium, hard mark different flight tasks.
- *TUM-VI*: The data comes from a hand-held device equipped with calibrated BMI160 IMU in different places and different motion modes. The ground truth is made by motion capture system but it only exists in a few sequences. So we use all six sequences with ground truth: Room 1-6.

B. Compared Methods

We compare the following approaches:

TABLE I
RELATIVE ORIENTATION ERROR(ROE) IN TERMS OF ORIENTATION(ROLL, PITCH AND YAW) IN DEGREE ON THE TEST SEQUENCE.

Dataset	Sequence	Roll			Pitch			Yaw		
		DIGDL	FSDA-F	FSDA	DIGDL	FSDA-F	FSDA	DIGDL	FSDA-F	FSDA
EuRoC	MH 04 difficult	14.8929	8.5595	8.0016	1.3958	-0.2955	-0.4349	-13.884	-6.954	-6.5309
	V2 02 medium	-36.0116	-29.2852	-30.1808	6.88	6.8074	6.321	34.9578	27.1108	28.1112
	V1 03 difficult	4.0002	0.0878	-0.6424	-0.9801	-1.8096	-1.1578	-5.041	-0.3453	-1.0451
	V1 01 easy	11.0515	4.2057	2.8124	1.3716	-1.3953	-1.2938	-9.249	-1.5872	-0.4603
	Absolute Average	16.4891	10.5346	10.4093	2.6569	2.577	2.3019	15.783	8.9993	9.0369
TUM-VI	Room2	-0.3668	0.7688	0.587	-1.844	-0.8445	-0.8855	8.9574	13.5548	10.3237
	Room4	0.3393	0.0081	0.1228	0.0971	-0.3237	-0.2693	15.7828	10.6631	9.4537
	Room6	-0.427	-0.0642	-0.2079	0.2103	0.1573	0.1517	9.8187	12.2971	8.8088
	Absolute Average	0.2833	0.2103	0.2294	0.5379	0.3314	0.3266	8.6397	9.1288	7.1466

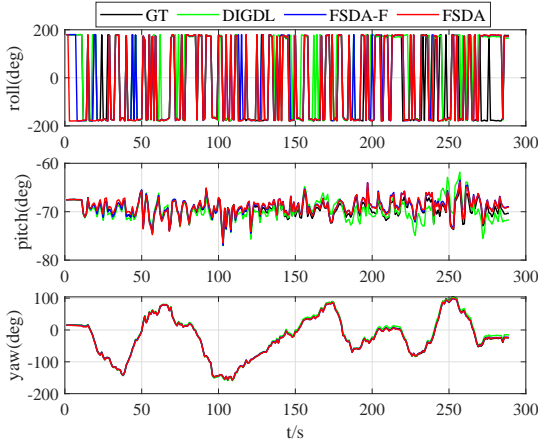


Fig. 7. Orientation estimates on the test sequence V1 01 easy for different methods.

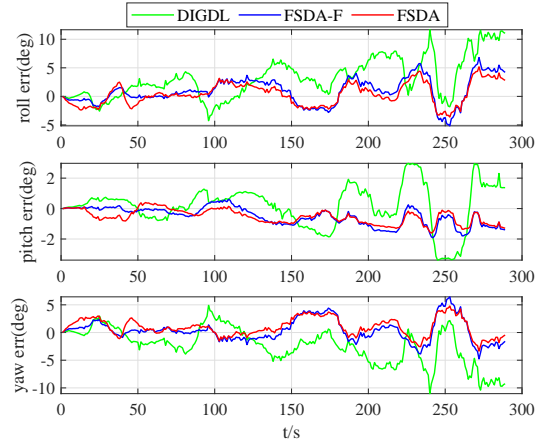


Fig. 8. Orientation errors on the test sequence V1 01 easy for different methods.

- GT: This is ground truth angular velocities.
- DIGDL: This method [17] beats top-ranked IMU denoising algorithms and visual-inertial odometry systems. Its training, validation and test sets are the same with our approach.
- FSDA-F: This is our framework without few-shot learning strategy for embedding module.
- FSDA: This is the proposed method.

C. Evaluation Metrics

We evaluate methods by Relative Orientation Error (ROE):

$$ROE = \|\log(\delta \mathbf{R}_n^T \delta \hat{\mathbf{R}}_n)\|_2 \quad (9)$$

The symbols in above equations are defined in denoising structure in session (III).

D. Results

In open datasets experiments, we set MH 01 easy, MH 02 easy, MH 03 medium, MH 05 difficult, V1 02 medium, V2 01 easy, V2 03 difficult from EuRoC, and room1, room3, room5 from TUM-VI as training sets and set MH 04 difficult, V1 01 easy, V1 03 difficult, V2 02 medium, room2, room4 and room6 as test sets. In each training set, data is divided

into two parts for learning and validation. Here learning part is for optimizing parameters and validation part is for evaluating bias.

From TABLE I, we first consider the denoising performance at the end of the sequence. Our proposed method performs 37.7% and 18.6% better than DIGDL respectively on EuRoC and TUM-VI in average. However, this results cannot evaluate the whole process since IMU sequence has large jitters, so we also need to see the denoising performance in whole IMU sequence. Fig. 5, 6, 7 and 8 represent the whole processing results for room4 and v1 01 easy. Obviously, FSDA and FSDA-F all perform better than DIGDL in all orientations. The comparison between FSDA and FSDA-F shows that few-shot learning strategy really works.

E. Interpreting the Embedding Module

The ability of our embedding module is qualified by the t-SNE projection (a tool to visualize high-dimension data) to show IMU sequences from multiple domains to an identical representation. The same t-SNE parameters (Perplexity=10, step=1000) are applied. As can be seen in Fig. 9, originally, data points from different domains are distinctly separated into four folds. However, after the representation of embed-

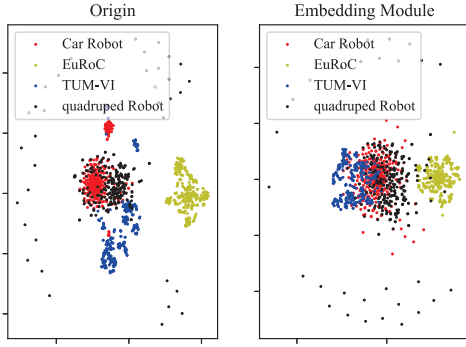


Fig. 9. Visualization of extracted representations of IMU sequence from different domains. Here, the EuRoC uses uncalibrated IMU.

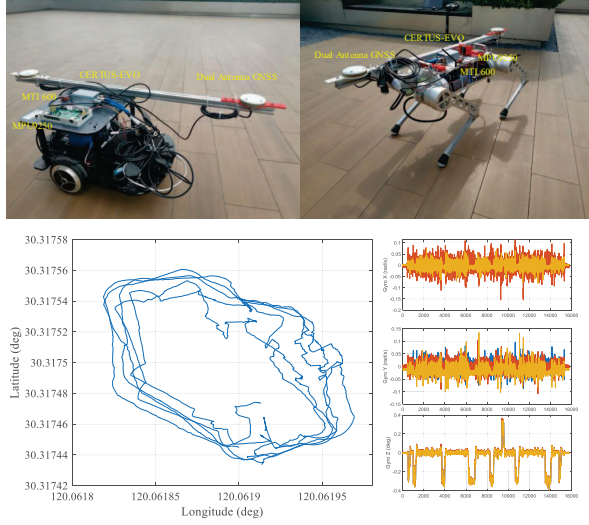


Fig. 10. Two robots (car on top left and quadruped robot on the top right), trajectories (on the down left) and three-axis angular velocity from gyroscopes

ding module, the data points are scattered more dispersively. Even for EuRoC (the uncalibrated IMU), the distributions of its data points has intersections with that of others. This verifies the effectiveness of embedding module and domain adaptability of our method.

F. Execution on real robots

We executed our few-shot domain adaptation method in two real robots and three different types of IMUs.

1) *IMU Setup*: We choose three IMUs with different precision. From high precision to low precision, they are CERTUS-EVO from ADVANCED NAVIGATION, MTI 600 series from XSSENS and MPU-9250 from TDK InvenSense:

- The CERTUS-EVO has the gyroscope with $0.2^\circ/hr$ bias instability, $6^\circ/hr/\sqrt{Hz}$ noise density and $< 0.03\%$ non-linearity, and accelerometer with $8\mu g$ bias instability, $2\mu g/\sqrt{Hz}$ noise density and $< 0.05\%$ non-linearity.
- The MTI 600 series has the gyroscope with $8^\circ/hr$ bias instability, $0.007^\circ/s/\sqrt{Hz}$ noise density and $0.1\%FS$ non-linearity, and accelerometer with $15\mu g$ bias in-

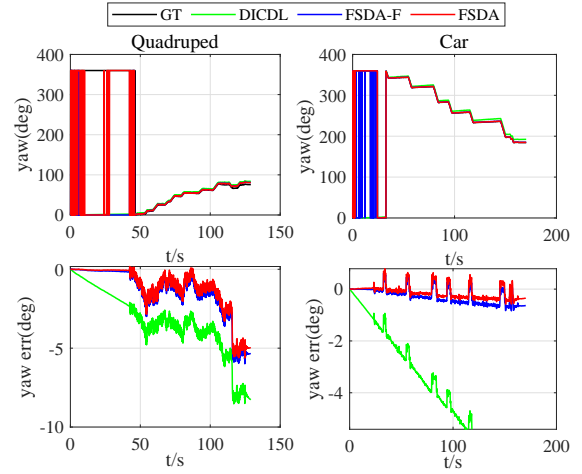


Fig. 11. Implementation on real robots

stability, $60\mu g/\sqrt{Hz}$ noise density and $0.1\%FS$ non-linearity.

- The MPU-9250 has the gyroscope with $0.01^\circ/s/\sqrt{Hz}$ noise density and $\pm 0.1\%$ non-linearity, and accelerometer with $300\mu g/\sqrt{Hz}$ noise density and $\pm 0.5\%$ non-linearity.

With dual antenna system, the CERTUS-EVO can also provide high-precision orientation which can be seen as ground truth.

2) *Robot Platform*: Two robot platforms are car and quadruped, which are set up as shown in 11.

In implementation, the car robot drives six times and each time it drove in a circle. The quadruped robot walked twice and each time it's trajectory was $3/4$ lap. Due to page limitation, we choose the yaw angle that is most likely to accumulate errors to show the performance of our method. The performance is shown in Fig. 11. As can be seen, our few-shot domain adaptation method works well on real robots and IMUs. Obviously, the divergence of the DICDL is serious, which means DICDL has no adaptability in sequence from different domains. Our FSDA framework drastically reduces the error. With the few-shot learning strategy, the performance is further improved.

V. CONCLUSION

To improve the IMU adaptability in multiple scenarios, we propose a few-shot domain adaptation method. To achieve the error of angular velocity, we propose a domain adaptation framework composed by embedding module, reconstructor module and generator module. The reconstitution loss is designed to improve domain adaptability. In addition, we adopt a few-shot training strategy for further improving the adaptability in the case of limited data. In the experiment, we first test our method on two datasets (EuRoC and TUM-VI). Performance is verified on the endpoint and the whole process of the sequence. We also implement our methods on two real robots with three kinds of IMUs. Besides, t-SNE is used to visualize the results of embedding module on datasets and real robots. This further proves the adaptability of our method.

REFERENCES

- [1] P. Zhang, J. Gu, E. E. Milios, and P. Huynh, "Navigation with imu/gps/digital compass with unscented kalman filter," in *IEEE International Conference Mechatronics and Automation*, 2005, vol. 3. IEEE, 2005, pp. 1497–1502.
- [2] W. Wang, Z. Wu, and H. Zhang, "An adaptive cascaded kalman filter for two-antenna gps/mems-imu integration," in *2018 IEEE/ION Position, Location and Navigation Symposium (PLANS)*. IEEE, 2018, pp. 833–837.
- [3] M. Karaim, A. Noureldin, and T. B. Karamat, "Low-cost imu data denoising using savitzky-golay filters," in *2019 International Conference on Communications, Signal Processing, and their Applications (ICCSPA)*. IEEE, 2019, pp. 1–5.
- [4] C. Jiang, S. Chen, Y. Chen, B. Zhang, Z. Feng, H. Zhou, and Y. Bo, "A mems imu de-noising method using long short term memory recurrent neural networks (lstm-rnn)," *Sensors*, vol. 18, no. 10, p. 3470, 2018.
- [5] Z. Wu and W. Wang, "Ins/magnetometer integrated positioning based on neural network for bridging long-time gps outages," *GPS Solutions*, vol. 23, no. 3, p. 88, 2019.
- [6] S. Han, Z. Meng, X. Zhang, and Y. Yan, "Hybrid deep recurrent neural networks for noise reduction of mems-imu with static and dynamic conditions," *Micromachines*, vol. 12, no. 2, p. 214, 2021.
- [7] H.-Y. Tseng, H.-Y. Lee, J.-B. Huang, and M.-H. Yang, "Cross-domain few-shot classification via learned feature-wise transformation," in *International Conference on Learning Representations*, 2020. [Online]. Available: <https://openreview.net/forum?id=SJl5Np4tPr>
- [8] S. Qiao, C. Liu, W. Shen, and A. L. Yuille, "Few-shot image recognition by predicting parameters from activations," in *Proceedings of the IEEE Conference on Computer Vision and Pattern Recognition*, 2018, pp. 7229–7238.
- [9] C. Finn, P. Abbeel, and S. Levine, "Model-agnostic meta-learning for fast adaptation of deep networks," in *International Conference on Machine Learning*. PMLR, 2017, pp. 1126–1135.
- [10] X. Zang, H. Yao, G. Zheng, N. Xu, K. Xu, and Z. Li, "Metalight: Value-based meta-reinforcement learning for traffic signal control," in *Proceedings of the AAAI Conference on Artificial Intelligence*, vol. 34, no. 01, 2020, pp. 1153–1160.
- [11] T. Jeong and H. Kim, "Ood-maml: Meta-learning for few-shot out-of-distribution detection and classification," *Advances in Neural Information Processing Systems*, vol. 33, 2020.
- [12] H. Liu, R. Socher, and C. Xiong, "Taming maml: Efficient unbiased meta-reinforcement learning," in *International Conference on Machine Learning*. PMLR, 2019, pp. 4061–4071.
- [13] T. Wang, Z. Wu, and D. Wang, "Visual perception generalization for visual-and-language navigation via meta-learning," *arXiv preprint arXiv:2012.05446*, 2020.
- [14] C. Q. Nguyen, C. Kretasoulas, and K. M. Branson, "Meta-learning gnn initializations for low-resource molecular property prediction," *arXiv preprint arXiv:2003.05996*, 2020.
- [15] L. Casas, A. Klimmek, G. Carneiro, N. Navab, and V. Belagiannis, "Few-shot meta-denoising," *arXiv preprint arXiv:1908.00111*, 2019.
- [16] S. Lee, D. Cho, J. Kim, and T. H. Kim, "Self-supervised fast adaptation for denoising via meta-learning," *arXiv preprint arXiv:2001.02899*, 2020.
- [17] M. Brossard, S. Bonnabel, and A. Barrau, "Denoising imu gyroscopes with deep learning for open-loop attitude estimation," *IEEE Robotics and Automation Letters*, vol. 5, no. 3, pp. 4796–4803, 2020.
- [18] F. Yu and V. Koltun, "Multi-scale context aggregation by dilated convolutions," in *International Conference on Learning Representations (ICLR)*, 2016.
- [19] M. Burri, J. Nikolic, P. Gohl, T. Schneider, J. Rehder, S. Omari, M. W. Achtelik, and R. Siegwart, "The euroc micro aerial vehicle datasets," *The International Journal of Robotics Research*, vol. 35, no. 10, pp. 1157–1163, 2016.
- [20] D. Schubert, T. Goll, N. Demmel, V. Usenko, J. Stückler, and D. Cremers, "The tum vi benchmark for evaluating visual-inertial odometry," in *2018 IEEE/RSJ International Conference on Intelligent Robots and Systems (IROS)*. IEEE, 2018, pp. 1680–1687.